

On-orbit rate normalization

Luca Baldini (luca.baldini@pi.infn.it)

August 14, 2010

Abstract

This is a short memo on the basic strategy we use to normalize the on-orbit LAT rates (with several different cuts applied) for the purpose of the data monitoring and the alarm system. The original implementation of the necessary code was put in place by David Panequie shortly after the launch. When we changed the rocking angle from 35° to 50° I made the necessary modifications to take into account the rate variations due to the change of the Earth limb arc length into the instrument field of view (especially in the selection with the highest photon content, namely the *source* and *diffuse* classes).

This note describe some of the work involved, along with additional modifications triggered by an excessive rate of spurious warnings during the rocking of the instrument that we started getting in the summer of 2010. The code necessary to produce the configuration files for the normalization code running in the pipeline is shortly described for future reference.

1 Introduction

As of August 14, 2010, the normalized rates are calculated by the data monitoring code running in the L1Proc pipeline based on the McIlwainL parameter and the rocking angle of the instrument. Some more details will be given in the following section. The purpose of this note is to describe possible improvements in order to avoid two specific issues which cause spurious alarms to trigger with a significant rate.

The first is a recurrent spike in the photon-rich data samples (most notably the diffuse class) corresponding to the rocking of the instrument (cfr. figure 1). This is due to the fact that, with a rock-

ing profile of 50° , the LAT has the Earth limb in the field of view for most of the time—except for the few minutes per orbit while it's rocking. When that happens, the photon-rich classes feature a decrease in the corresponding rate which must be properly taken into account (the contribution of photons from the Earth limb is negligible in the background-dominated data samples, so this is less of an issue for the selection with a high background content).

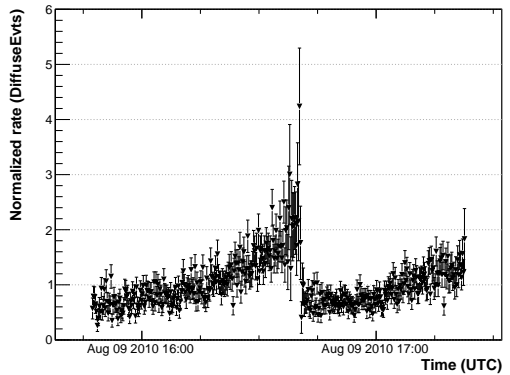


Figure 1: Normalized rate for the diffuse class events for run 0303054436. The spike in the middle of the run correspond to the rocking of the instrument.

The second issue is a recurrent dip for the background-dominated data samples occurring, as we shall see, at a specific longitude in the orbit of the observatory (cfr. figure 2) and most likely related to the South Atlantic Anomaly (in fact the recurrence of the dip is modulated according to the SAA epoch).

Both aspects will be discussed with more details in the following sections.

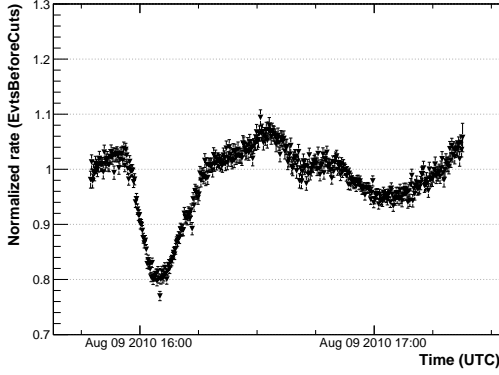


Figure 2: Normalized rate for the events before any cut for run 0303054436. As we shall see, the dip close to the beginning of the run is characteristic of a particular spot in the orbit and can be (at least partially) corrected for.

2 McIlwain L normalization

The first (and most prominent) correction is the one taking into account the McIlwain L geomagnetic parameter.

The starting point is a root tree in which the merit trending product for a long time span (typically 56 days) are merged together (details on how to produce such a tree will be given in the next sections). An histogram of the `Mean_PtMcIlwainL` variable is created requiring that the rocking zenith angle θ_r is close (typically within 0.2°) to 50° . The for each rate variable another histogram is made (with the same cut) and the latter is divided by the first one. The procedure (the result is shown in figure 3 for two different selections) is equivalent to the calculation of the average rate (for each selection) in each McIlwain L bin (with unit weight).

For each bin in such histograms the bin content gives the number the corresponding rate must be divided by to get the normalized rate (at 50° rocking angle) in each McIlwain L bin (for historical reasons the information in the output text file is stored in the form of a global average value and the relative bin-to-bin corrections, but this is substantially irrelevant). The basic idea is that this first step takes care of the geomagnetic dependence at the tipical rocking angle and the additional variations are taken care of in successive steps.

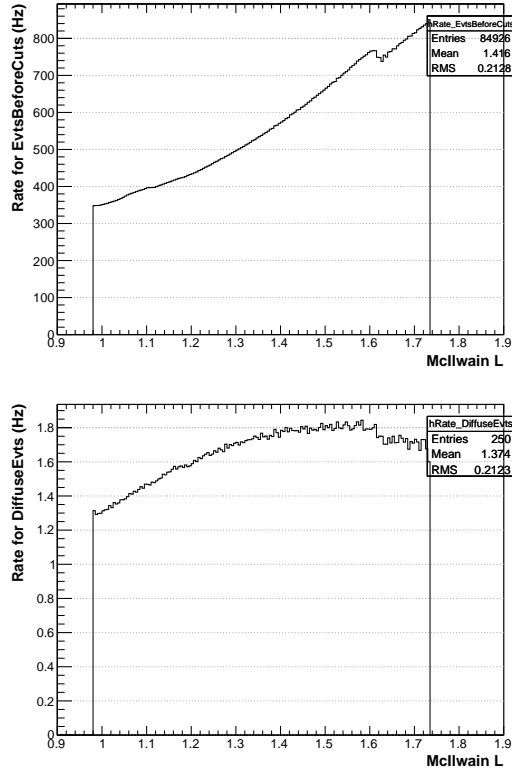


Figure 3: Dependence of the event rate on the McIlwain L parameter for two different selections: before any cut (top panel) and after the diffuse cuts (bottom panel).

3 The Earth limb in the FOV

Next comes the normalization for the Earth limb in the field ov view. In the original implementation the dependence of the various rates on the rocking angle (for $\theta_r \neq 50^\circ$) was fitted (with no additional cut) with a polinomial of third degree. The choice of the fitting function was, retrospectively, a bad choice, as in general the best fit featured a concavity in the regin $0^\circ \leq \theta_r \leq 40^\circ$, where the Earth limb is outside the field of view and therefore the event rates should be approximately constant. Another issue was due to the fact that for the low-background event classes (most notably the diffuse class) the absolute average rate is low—typically of the order of ≈ 0.2 Hz when the limb is outside the field of view. As a consequence the number

of counts in a 15 s time bin is also low (≈ 3) and the corresponding Poisson fluctuation (especially toward high values) can be noticeable.

The new implementation constitutes an attempt to overcome this limitation. The functional form of the new fitting function is:

$$f(\theta_r) = \begin{cases} c_0 & \theta_r < 35^\circ \\ c_0 + c_1\theta_r + c_2\theta_r^2 & \theta_r > 35^\circ \end{cases} \quad (1)$$

i. e. it is a constant when the limb is outside the field of view with the addition of a second order polynomial to parametrize the effect of the limb itself. On top of that, a cut of the normalized rate (i. e. rate normalized for the McIlwain L) is performed before the fit, requiring that the rate itself is greater than 0.3 (adjustable). This has small or no effect for most of the event classes and constitutes a rough but effective way to artificially increase the average for the low-rate classes (i. e. diffuse and source) and suppress the effect of the Poisson fluctuations toward high values.

An example of such a fit (for the diffuse selection, which at this stage is the most critical one) is presented in figure 4.

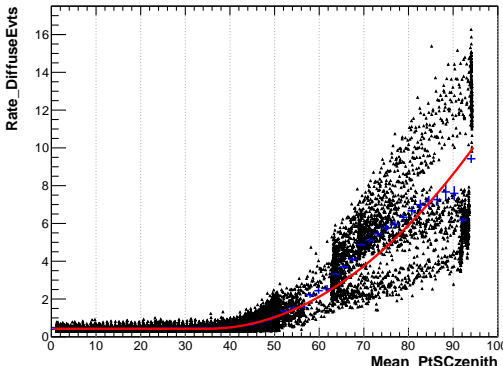


Figure 4: Fit of the rocking angle dependence of the diffuse class rate (after the normalization for the McIlwain L dependence). Each point is a time bin (for a total of 56 days) and the time bins with a normalized rate lower than 0.3 have been removed prior to the fit. The blue histogram is a profile of the underlying two dimensional histogram and the red line is a fit to such a profile. Note that the fit value is very close to 1 for $\theta_r = 50^\circ$.

The effect of the new implementation on an actual run is shown in figure 5, which can be compared directly with figure 1. The improvement is evident, with the highest data point going down from ≈ 4.5 to ≈ 2.5 .

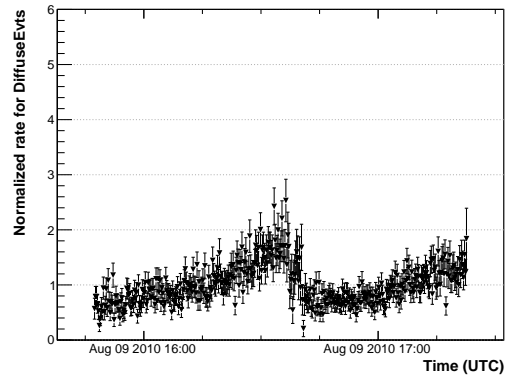


Figure 5: New normalized rate for the diffuse class events for run 0303054436 (compare with figure 1). The spike in much less prominent with the new algorithm.

4 The longitude modulation

The last issue is the recurrent dip in normalized rate (after the McIlwain L and the Earth limb corrections) in the background-dominated classes. It appears that, among all the geographic or geomagnetic variables, such dip feature the highest correlation with the geographic longitude (cfr. figure 6).

The correlation is fitted with a triangular function:

$$f(\theta_r) = \min(1, 1 - c_0 + c_0|c_2(x - c_1)|) \quad (2)$$

where c_0 (the amplitude of the variation) is of the order of 15% for event rate before any cut and is much less pronounced for the photon-rich classes—for which, in fact, it is disengaged.

The effect of such a correction is shown in figure 7, which can be compared directly with the original implementation (in which such a correction was not applied) in figure 2.

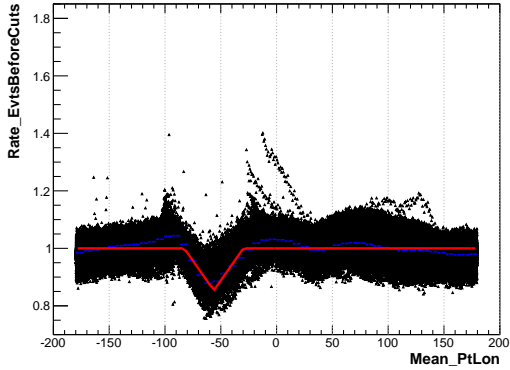


Figure 6: Dependence of the normalized rate of events before the cuts on the geographies longitude.

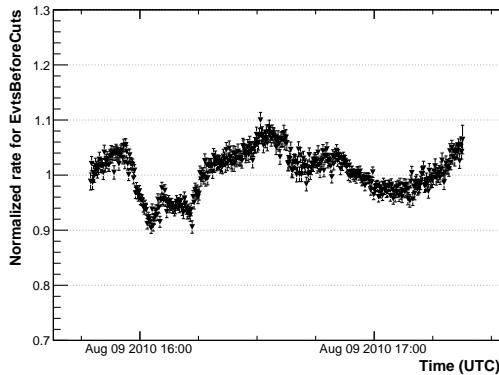


Figure 7: New normalized rate for the events before any cut for run 0303054436, after the longitude correction has been applied (cfr. figure 2).

After this new correction the overall normalized rate (at least for this run) is consistent with unity to 10% and the dip is much less prominent.

5 Running the code

All the code needed in order to generate the configuration files for the rate normalization lives in the cvs area `dataMonitoring/Tools/python`.